Applied Catalysis B: Environmental 84 (2008) 773–782

Contents lists available at ScienceDirect

Applied Catalysis B: Environmental

journal homepage: www.elsevier.com/locate/apcatb

Pt-CeO_2/C anode catalyst for direct methanol fuel cells

M. Aulice Scibioh, Soo-Kil Kim, Eun Ae Cho, Tae-Hoon Lim, Seong-Ahn Hong, Heung Yong Ha *

Center for Fuel Cell Research, Korea Institute of Science and Technology, P.O. Box 131, Cheongryang, Seoul 130-650, South Korea

ARTICLE INFO

Article history:
Received 1 February 2008
Received in revised form 26 May 2008
Accepted 11 June 2008
Available online 26 June 2008

Keywords:
CeO_2-modified Pt/C catalyst
Cyclic voltammetry
Methanol oxidation
Direct methanol fuel cell

ABSTRACT

In order to develop a cheaper and durable catalyst for methanol electrooxidation reaction, ceria (CeO_2) as a co-catalytic material with Pt on carbon was investigated with an aim of replacing Ru in PtRu/C which is considered as prominent anode catalyst till date. A series of Pt-CeO_2/C catalysts with various compositions of ceria, viz. 40 wt% Pt-3–12 wt% CeO_2/C and PtRu/C were synthesized by wet impregnation method. Electrocatalytic activities of these catalysts for methanol oxidation were examined by cyclic voltammetry and chronoamperometry techniques and it is found that 40 wt% Pt-9 wt% CeO_2/C catalyst exhibited a better activity and stability than did the unmodified Pt/C catalyst. Hence, we explore the possibility of employing Pt-CeO_2 as an electrocatalyst for methanol oxidation. The physicochemical characterizations of the catalysts were carried out by using Brunauer Emmett Teller (BET) surface area and pore size distribution (PSD) measurements, X-ray diffraction (XRD), X-ray photoelectron spectroscopy (XPS) and transmission electron microscopy (TEM) techniques. A tentative mechanism is proposed for a possible role of ceria as a co-catalyst in Pt/C system for methanol electrooxidation.

1. Introduction

Direct methanol fuel cells (DMFCs) are now being considered as attractive power sources for portable power and electric vehicle applications. In a DMFC, it is methanol oxidation at the anode catalyst rather than oxygen reduction at the cathode catalyst that limits the performance of the fuel cell [1]. The main reason for DMFC anode rate limitation is apparently the sluggish electro-oxidation of adsorbed carbon monoxide, an intermediate product of anodic methanol oxidation [2,3]. Efforts to mitigate CO poisoning have been attempted through the addition of co-catalysts to platinum such as Ru [4–15], Mo [16,17], Sn [17], W [17,18], Nb [19], Ni [20–23]. Binary Pt–Ru alloys are still considered as state of the art catalysts for methanol oxidation in DMFC. Ruthenium crossover [24] has triggered serious concerns about anode materials stability among researchers and developers of DMFCs. In addition to the element to be added to Pt, several authors have shown that the addition of oxides to metallic Pt (PtM_yO_x, where M = Sn, Mo, Os or W) is efficient [25,26]. It has been suggested that the oxides are capable of adsorbing large quantities of OH species, which are involved in the oxidation/reduction mechanisms taking place between the different possible oxidation states of the metal oxides [27]. Addition of transition metal oxides (MoO_x, VO_x and WO_x) to PtRu has also been attempted by a few researchers for an enhanced methanol oxidation reaction (MOR) [28–31], and they demonstrated that these modified catalysts yielded a higher methanol oxidation current than the conventional PtRu catalysts. For DMFC anode catalyst performance improvement, the exploration of new catalyst materials including noble and non-noble metals is necessary. In this respect, an alloying strategy is one of the R&D directions.

Regarding cost reduction for early DMFC commercialization, DMFC anode catalyst loadings must drop to a level of < 1.0 mg cm^{-2} from the present 2.0–8.0 mg cm^{-2}, depending on applications. Loading reduction through increasing Pt utilization is one of the approaches. Non-noble catalyst development is another approach for catalyst cost reduction. A more thorough exploration is needed in DMFC anode catalysis with respect to performance, durability and cost.

Some noble metal loaded ceria catalysts have received considerable attention because they are used in automobile catalytic converters [32]. Ceria is widely regarded as a kind of oxygen tank to adjust oxygen concentration at the catalyst surface under reaction condition. Ceria has a fluorite structure whose cations can switch between +3 and +4 oxidation states and it has the ability to act as an oxygen buffer [33]. It has been reported that interaction between noble metal such as Pt with ceria enhances the catalytic activities. The promoting action of CeO_2 is attributed to oxygen storage capacity (OSC) at low temperature, higher reducibility in the presence of Pt, higher dispersion of Pt over CeO_2 and prevention of sintering of Pt metal particles [34]. Yu et al. [35] has reported that the incorporation of an oxygen storage

* Corresponding author. Tel.: +82 2 958 5275; fax: +82 2 958 5199.
E-mail address: hyha@kist.re.kr (H.Y. Ha).

0926-3373/$ – see front matter © 2008 Elsevier B.V. All rights reserved.
doi:10.1016/j.apcatb.2008.06.017

material such as ceria (CeO_2) into the cathode catalyst increased the local oxygen concentration in the air atmosphere, leading to an enhancement in the performance of a DMFC. Recently, Xu and Shen [36,37] reported on electrochemical oxidation of methanol, ethanol, glycerol and ethylene glycol on Pt-CeO_2/C in alkaline media showing an improved performance compared to Pt/C catalysts. Campos et al. [38] adopted occlusion deposition method to prepare Pt/CeO_2 on a glassy carbon (GC) electrode under a constant potential in a bath solution containing both ceria and K_2PtCl_6. They found an increased catalytic activity for methanol oxidation with the ceria composite electrode in comparison to Pt/C system. However, both of these studies lack detail physicochemical characterization of catalysts and information on mechanistic details. Guo et al. [39] have employed PtRu-CeO_2/C catalyst synthesized by sodium borohydride reduction route and found that a particular composition namely $PtRu_{0.7}(CeO_2)_{0.3}$/C yielded a higher methanol oxidation current than the unmodified PtRu/C catalyst.

In the present investigation, we employed CeO_2 as a co-catalytic material in Pt/C catalyst based on the fact that CeO_2 has a higher OSC [40]. It is expected that the oxygen atoms present in the lattice of CeO_2 can either directly or indirectly involved in promoting the CO removal which is formed on Pt during the electrooxidation of methanol. However, at this stage we have not ruled out the possible electronic effect of ceria on Pt in weakening CO bond. Ru presence has been completely avoided in the catalyst in spite of its better activity due to three reasons. The first one is that, we want to reduce the noble metal loading for cost reasons as Ru is also a noble metal. The second one is that Ru seems like leaching out in the long term operations [24], and hence imposing severe constraints on practical applications and reliable performance. The third one is that we want to exclusively understand the role of ceria in CO removal in fuel cell catalyst in the absence of Ru which also plays a major role in this poisoning removal.

In order to understand the possible role of ceria as a co-catalytic material, we have synthesized 40 wt% Pt-CeO_2/C with different compositions of ceria (3–12 wt%). Electrocatalytic activity of these catalysts towards the methanol oxidation reaction was examined by using cyclic voltammetry (CV) and chronoamperometry techniques. Physicochemical characterizations of the catalysts were also made by using various techniques.

2. Experimental

2.1. Preparation of 40 wt% Pt-3–12 wt%(CeO_2)/C nanocatalysts

At first, CeO_2/C was made by taking the required amount of Ce $(NO_3)_3{\cdot}6H_2O$ dissolved in water and by adding this solution drop wise to carbon black powder (Vulcan XC-72R, Cabot) dispersed in water under thorough mixing by using mechanical stirrer under 80 °C heating for nearly 6 h until the complete evaporation of water, followed by drying overnight in oven at 70 °C. The resulting material was calcined in nitrogen atmosphere at 1200 °C for 2 h with a heating rate of 5 °C/min to obtain CeO_2/C. To make Pt-CeO_2/C nanocatalysts by wet impregnation method, CeO_2/C was well dispersed in water and to this solution, required amount of $H_2PtCl_6{\cdot}6H_2O$ in water was added drop wise under constant stirring followed by complete evaporation of water and dried overnight in oven. The resulting material was reduced in hydrogen atmosphere at 300 °C for 2 h (heating rate = 5 °C/min) to obtain 40 wt% Pt-3–12 wt% (CeO_2)/C nanocatalysts. The catalyst composition is described as follows. We made 40% Pt on ceria/C support, assuming the total amount is 100 g, in which Pt = 40 g, ceria + C = 60 g. The ceria content was varied by maintaining the Pt wt% same in all catalyst systems. The ceria content was 3, 6, 9 and 12 g in catalysts 40–3% CeO_2/C, 40–6% CeO_2/C, 40–9% CeO_2/C and 40–12% CeO_2/C, respectively, and the catalysts are accordingly designated as PC3, PC6, PC9 and PC12, respectively. The Pt-Ru/C supported catalysts were prepared according to wet impregnation method (PR-Imp) by using $H_2PtCl_6{\cdot}6H_2O$ and $RuCl_3$ as precursors with the atomic ratio of Ru to Pt as 50:50.

2.2. Physico-chemical characterization

The chemical compositional analyzes were conducted for the presence of appropriate amount of platinum, ceria and carbon in all prepared catalyst systems by using inductively coupled plasma technique and the results were consistent with the catalyst compositions. The surface morphologies of the catalyst systems were examined by transmission electron microscopic (TEM) technique using a Phillips–CM30 electron microscope. X-ray diffraction (XRD) measurements were recorded on Rint-Dmax 2500, Rigaku instrument, using a nickel-filtered CuKα (0.15418 nm) source. Scans were acquired with 0.02° step size over 2θ range 10–90°. Average crystallite size was estimated with the help of the Debye–Scherrer equation, using the XRD data of prominent lines. Brunauer Emmett Teller (BET) surface area, pore size distribution (PSD) and pore volume were measured by the physisorption method using nitrogen at liquid nitrogen temperature using a Micromeritics ASAP 2010 analyzer. The specific surface area S_{BET} was determined from the linear portion of the BET plot. The PSD was calculated from the adsorption and desorption branch of the N_2 adsorption isotherm using the Barrett–Joyner–Halenda (BJH) formula. The total pore volume was calculated by means of the total amount of adsorbed gas at $P/P_0 = 0.98$. Prior to the surface area and PSD measurements, the samples were degassed in vacuum at 573 K for 3 h to remove physically adsorbed components. The X-ray photoelectron spectroscopy (XPS) measurements of the PtCeO_2/C nanocatalysts were carried out with a Physical Electronics PHI 5600 multi-technique system using an Al monochromatic X-ray at a power of 350 W. The regional XPS of Pt_{4f} and Ce_{3d} spectra were deconvoluted by using the multipak software to identify different oxidation states of Pt on carbon. The binding energies were calibrated with respect to the signal of carbon (284.6 eV).

2.3. Electrochemical measurements in a half cell

The cyclic voltammetry studies were carried out in a conventional airtight three-electrode cell containing aqueous solution of 0.5 M in H_2SO_4 and 1.0 M methanol at 25 °C at a scan rate of 50 mV/s. Thin film electrodes were prepared by dispersing 20 mg of PtCeO_2/C in deionized water and isopropyl alcohol, ultrasonicating for 30 min, and pipeting out 10 μL of the resulting suspension on a glassy carbon substrate (0.307 cm^2 surface) using a micropipette followed by drying in air and adding 5 μL of 5% Nafion solution as a binder to affix the electrocatalysts firmly to the GC, the solvent was allowed to evaporate slowly. Prior to making measurements with the cyclic voltammetry and chronoamperometry experiments, the electrolyte was purged with nitrogen gas for 2 h. Chronoamperometry data were collected for 1 h at 0.5 V versus SCE (saturated calomel electrode) for the catalysts in a mixture of 0.5 M H_2SO_4 as electrolyte and 1.0 M methanol solution at 25 °C. Impedance measurements were conducted immediately after chronoamperometry tests by sweeping the frequency from 5000 to 0.050 Hz in a constant voltage mode at an amplitude of 10 mV. All electrochemical experiments were made by using Autolab instrument.

Electrochemical active surface area (ESA) of the catalysts was measured by CO_{ad} stripping voltammetry in 0.5 M H_2SO_4 solution at a scan rate of 50 mV/sec. For CO stripping measurements, pure

CO was bubbled into the electrolyte for 10 min and its adsorption on the electrode was driven under potential control at 150 mV versus SCE for 120 s. The electrolyte was purged for 30 min with nitrogen, keeping electrode at open circuit potential to eliminate CO reversibly adsorbed on the surface. The electrochemical active area of the catalyst particles was determined assuming the formation of a monolayer of linearly adsorbed CO and the Columbic charge required for oxidation of CO_{ad} to be 484 μC cm^{-2} [41–44].

3. Results and discussion

Cyclic voltamograms in a half cell configuration for methanol oxidation were at first recorded for both commercial and home-made catalyst systems such as 40 wt% Pt/C and 40 wt% PtRu/C (Fig. 1a) to evaluate whether our catalyst preparation procedure is good. The home-made catalysts (PC0 and PR-Imp) showed comparable activities towards methanol oxidation reaction with those of commercial E-Tek catalysts (P-ET and PR-ET). The electrocatalytic activities of 40 wt% Pt- CeO_2/C catalysts with varied ceria composition (0, 3, 6, 9 and 12 wt% are designated as PC0, PC3, PC6, PC9, and PC12, respectively) and a PtRu/C catalyst prepared by wet impregnation method (PR-Imp) towards the oxidation of methanol were tested by using cyclic voltamograms as shown in Fig. 1b. It can be seen that the onset potential of Pt/C (P-ET or PC0) catalysts starts nearly at 480 mV/NHE. The onset potentials of PC0, PC3 and PC6 (478, 476 and 475 mV/NHE respectively) appear to be closer to each other though there is a slight increase in current density with PC6 system indicating that

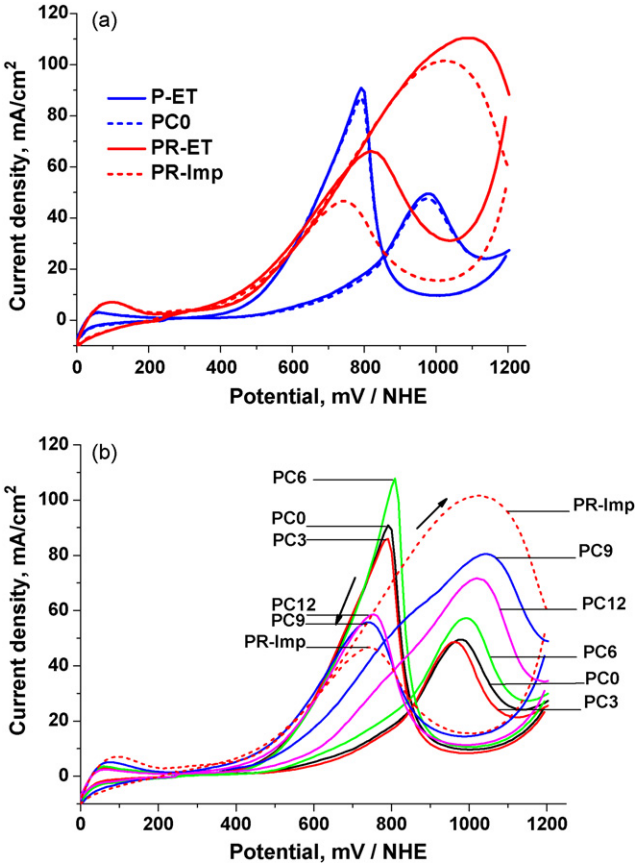

Fig. 1. Cyclic voltamograms of methanol oxidation on catalyst systems (a) PR-Imp, PR-ET, P-ET and PC0 (b) PC0, PC3, PC6, PC9, PC12 and PR-Imp in a mixture of 0.5 M H_2SO_4 + 1.0 M methanol solution at 25 °C at a scan rate of 50 mV/s.

when ceria is present in lower amounts, it has no pronounced influence on methanol oxidation activity. However, the onset potentials of PC6 and PC8 start at around 412 and 415 mV/NHE, respectively, which are nearer to the onset potential of PtRu/C system starting at around 375 mV/NHE. The electrocatalytic properties of various catalyst systems under this study including the typical on-set potentials are enlisted in Table 1.

The peak current density values from cyclic voltamograms of these catalyst systems towards electrooxidation of methanol (Fig. 1) are in the order: PC0 ~ PC3 < PC6 < PC9 > PC12. The voltammetric features are consistent with literature reports and are typical of the electrooxidation of methanol on Pt-based bimetallics [45–48] namely: a methanol oxidation peak during the forward scan (from 0 to 1.2 V) occurs at about 1000 mV (versus normal hydrogen electrode, NHE) and another anodic peak on the reverse scan (~750 mV versus NHE) due to the removal of incompletely oxidized carbonaceous species formed in the forward scan [49,50].

A method to benchmark the catalyst performance is to compare the ratio of current densities associated with the anodic peaks in the forward (I_f) and reverse (I_b) scans. Such a ratio has been used to infer the CO tolerance of the catalysts [49,50]. A lower I_f/I_b value signifies poor oxidation of methanol to CO during the anodic scan and excessive accumulation of carbonaceous species on the catalyst surface: in other words, a greater extent of CO poisoning (Table 1). Hence, a higher I_f/I_b value is indicative of improved CO tolerance. It can be seen that peak patterns of PC0, PC3 and PC6 appear similar to that of Pt/C catalysts with lower forward to backward peak height ratio, indicating the CO poisoning [51]. However, the I_f/I_b values of PC9 and PC12 become much higher than those of PC3 and PC0 and their peak patterns resembles PtRu/C system with reduced backward peak height compared to forward peak. From this, it is speculated that ceria assists in the removal of the CO, an intermediate poisonous moiety formed during methanol electrooxidation and thus behaves similar to Ru in PtRu system. At low ceria content, there are not enough ceria sites to effectively assist the release of adsorbed CO_{ads} and the oxidation current remains almost at the same level obtained from pure platinum on carbon catalyst. While increasing the ceria content, the current density increases, but the excess amount of ceria (PC12) leads to a lower activity. It is not clear what kind of resistance is there, and the performance drops after the optimum level (PC9).

The chronoamperometric technique is an effective method to evaluate the electrocatalytic activity and stability of electrode material. Fig. 2 shows typical current density-time responses for methanol oxidation measured at a fixed potential of 0.742 V/NHE (0.5 V/SCE) of all catalyst systems supported on carbon electrodes in 0.5 M H_2SO_4 aqueous solution containing 1.0 M CH_3OH [52]. As

Table 1
Comparison of electrocatalytic properties of the catalysts

Catalyst	On-set potential (mV/NHE)	Peak current density (mA/cm^2)	I_f/I_b
P-ET	480	49	0.54
PC0	478	49	0.54
PC3	476	48	0.55
PC6	475	56	0.53
PC9	412	80	1.45
PC12	415	71	1.23
PR-Imp	375	102	2.17
PR-ET	378	101	2.16

P-ET – 40 wt% Pt/C (E-Tek), PR-ET – 40 wt% PtRu/C (E-Tek), PR-Imp – 40 wt% PtRu/C (impregnation method of preparation), I_f–current density associated with anodic peak in forward scan and I_b–current density associated with anodic peak in reverse scan.

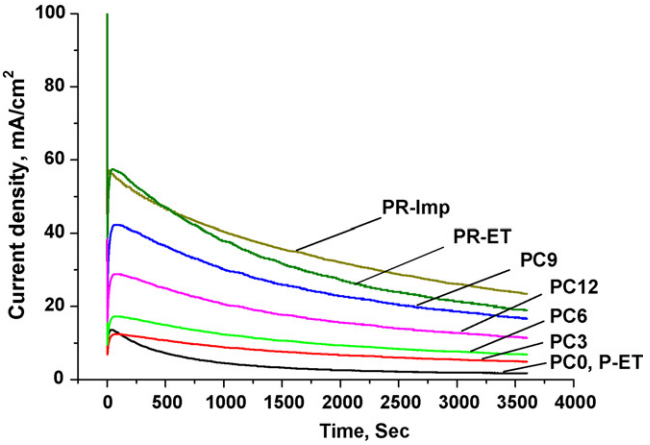

Fig. 2. Chronoamperometry data collected for 1 h at 0.5 V versus SCE for the catalyst systems in aqueous solution of 0.5 M H_2SO_4 + 1.0 M methanol at 25 °C.

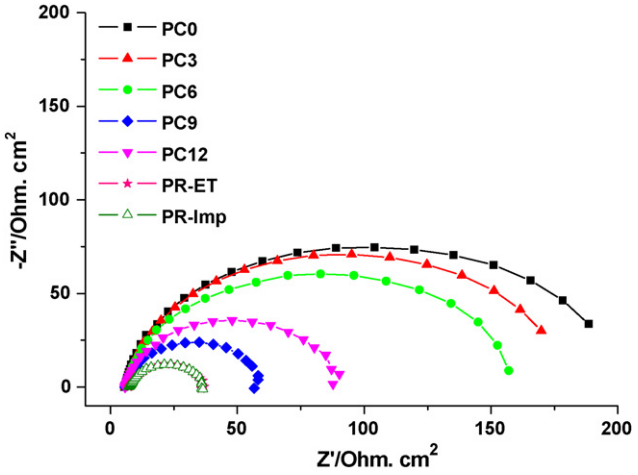

Fig. 3. Nyquist plots for catalyst systems such as PC0, PC3, PC6, PC9, PC12, PR-ET and PR-Imp in aqueous solution of 0.5 M H_2SO_4 + 1.0 M methanol at 25 °C.

expected, the methanol oxidation current at PR-Imp and PR-ET was evidently higher than Pt-ceria or Pt alone systems. These results indicate that the PtRu/C system has a higher activity than Pt-ceria or Pt alone systems. The methanol electro-oxidation current in all ceria containing Pt systems was greatly enhanced compared to Pt alone system. The PC0 and Pt/C-ETek (P-ET) catalysts showed exactly the same performance drop during the first 1 h of study and hence only PC0 is shown in the figure. It is apparent that the drop in activity is less in ceria incorporated Pt/C catalysts compared to ceria free PC0 (Pt/C) catalysts. Both the cyclic voltammetry and chronoamperometric data show that Pt-CeO_2/C catalysts are more effective for the methanol oxidation than Pt/C catalysts.

Electrochemical impedance spectroscopic (EIS) studies have been carried out to investigate the intrinsic behavior of the anodic process. Compared to the studies with full membrane electrode assembly in which hydrogen is passed on the cathode side, the electrolyte resistance in the impedance data could be avoided and anodic process can be examined with accuracy in a half-cell configuration. Fig. 3 shows the complex impedance plots for catalysts in 0.5 M H_2SO_4 + 1.0 M MeOH aqueous solution in a potentiostatic mode of 0.742 V/NHE (0.5 V/SCE). The Nyquist plots consist mainly of semicircles, whose diameters are associated with the charge transfer resistance indicating the catalytic activity for methanol oxidation reaction [53]. The impedance plot of PC0 and Pt/C-ETek (P-ET) appears to be same and hence only PC0 is shown. It can be seen that compared to Pt/C system, the diameters of semicircles in case of PtRu/C systems (PR-ET, PR-Imp) are very small showing the facile methanol oxidation with PtRu/C system unlike with Pt/C system. The ceria addition to Pt/C appears to decrease the charge transfer resistance than Pt0 and a minimum is found with PC9 system, indicating an improved methanol oxidation activity by ceria. We in fact anticipated a kind of Ohmic resistance by the addition of ceria in the catalyst but until 9 wt% of ceria we have not found any Ohmic resistance. This may be attributed to the increased electrical conductivity of nanophase ceria compared to bulk ceria [54]. However, further addition of ceria to Pt/C system increases the charge transfer resistance. EIS studies provide an additional evidence for the promoting effect of ceria. The shrinkage in diameter of semicircles in Nyquist plots reflect the improved catalytic activities of ceria incorporated platinum catalysts which is in accordance with catalytic activities inferred from cyclicvoltammetric studies (Fig. 1b).

The methanol oxidation process should involve many parallel processes with reaction intermediates. In this study, the impedance data can be analyzed assuming two major reactions; namely the CH_3OH to CO_{ad} and CO_{ad} to CO_2. The curls observed in the lower frequency regions of PC6 and PC8 may be attributed to the pseudo-inductive behavior [55–57] due to CO_{ad} oxidation as in case with PtRu. A straight line at high frequencies, a capacitive loop at medium frequencies and an inductive loop at low frequencies observed in case with PC9 and PC12 are similar to PtRu, which indicates the mechanism may be similar in these cases.

The ESA of the catalyst systems was determined by CO_{ad} stripping voltammetry, assuming the formation of a monolayer of linearly adsorbed CO and the coulombic charge required for oxidation of CO_{ad} to be 484 μC cm^{-2} (Table 2). The ESAs for Pt/C-ETek (P-ET) and PC0 are 48 and 50 m^2/g, respectively. The typical ESA values calculated for the systems such as PC3, PC6, PC9 and PC12 are 53, 55, 60 and 57 m^2/g, respectively. ESA of ceria doped Pt/C catalysts increases with increasing ceria content and shows a maximum value for PC9. Since CO species are the main poisoning intermediate in electro-oxidation of methanol while employing platinum catalysts, a co-catalyst may assist the removal of the poisoning intermediate and thus offering excellent CO electro-oxidizing ability to the catalyst system, and this quality can also be studied by using CO stripping tests. This information may help to analyze the mechanism behind the enhanced electro-catalyzing activity of Pt-CeO_2/C catalysts for methanol electro-oxidation (as shown in Fig. 1). Fig. 4 presents the CO-stripping voltamograms of ceria free and ceria incorporated platinum supported catalyst systems studied in this present investigation. The onset stripping potential and the peak maxima are tabulated in Table 3, which may directly reflect the CO-oxidizing ability of the catalysts. It can be seen that in ceria incorporated platinum supported catalysts such as PC3, PC6, PC9 and PC12, the on-set potential and peak maxima are shifted to lower potentials compared to ceria free commercial (P-ET) as well as home-made (PC0) Pt alone systems, as shown in Fig. 4.

Table 2
Results of XRD, TEM and ESA of the catalysts

Catalyst	Particle size (nm) XRD (TEM)	ESA (m^2/g)
P-ET	4.5 (4.0)	48
PC0	4.2 (3.7)	50
PC3	4.0 (3.5)	53
PC6	4.0 (3.5)	55
PC9	3.5 (3.0)	60
PC12	3.6 (3.0)	57
PR-Imp	4.0 (3.5)	61
PR-ET	2.9 (2.6)	63

*ESA from CO stripping.

Table 3
Comparison of CO-stripping properties of the catalysts

Catalyst	On-set potential (mV/NHE)	Peak maxima (mV/NHE)
P-ET	596	796
PC0	594	782
PC3	559	765
PC6	557	764
PC9	556	764
PC12	557	765

*P-ET – 40 wt%Pt/C (E-Tek).

The supported electrocatalysts under this study were subjected to morphological and physico-chemical characterization tests such as transmission electron microscopy, X-ray diffraction, BET–PSD surface area measurements and X-ray photoelectron spectroscopy.

Fig. 5 presents the transmission electron micrographs of PC0 (Pt/C), and all ceria incorporated Pt/C under this study namely PC0, PC3, PC6, PC9 and PC12 as well commercial and home-made PtRu/C (PR-ET and PR-Imp) catalysts. The catalyst particles are homogeneously dispersed with no much pronounced agglomerations in case of Pt/C with and without ceria incorporations. Table 2 lists the average particle sizes measured from randomly selected 100 particles in each catalyst system from TEM studies. The 40 wt% Pt/C (E-Tek) catalyst exhibited platinum particle sizes of around 4 nm, whereas the home-made 40 wt% Pt/C showed the platinum particle sizes around 3.7 nm. PC2 and PC4 showed the platinum particle sizes of around 3.5 nm, while PC6 and PC8 showed the particle sizes around 3.0 nm. The ceria incorporation slightly decreases the size of platinum particles in all Pt-CeO_2/C catalyst systems.

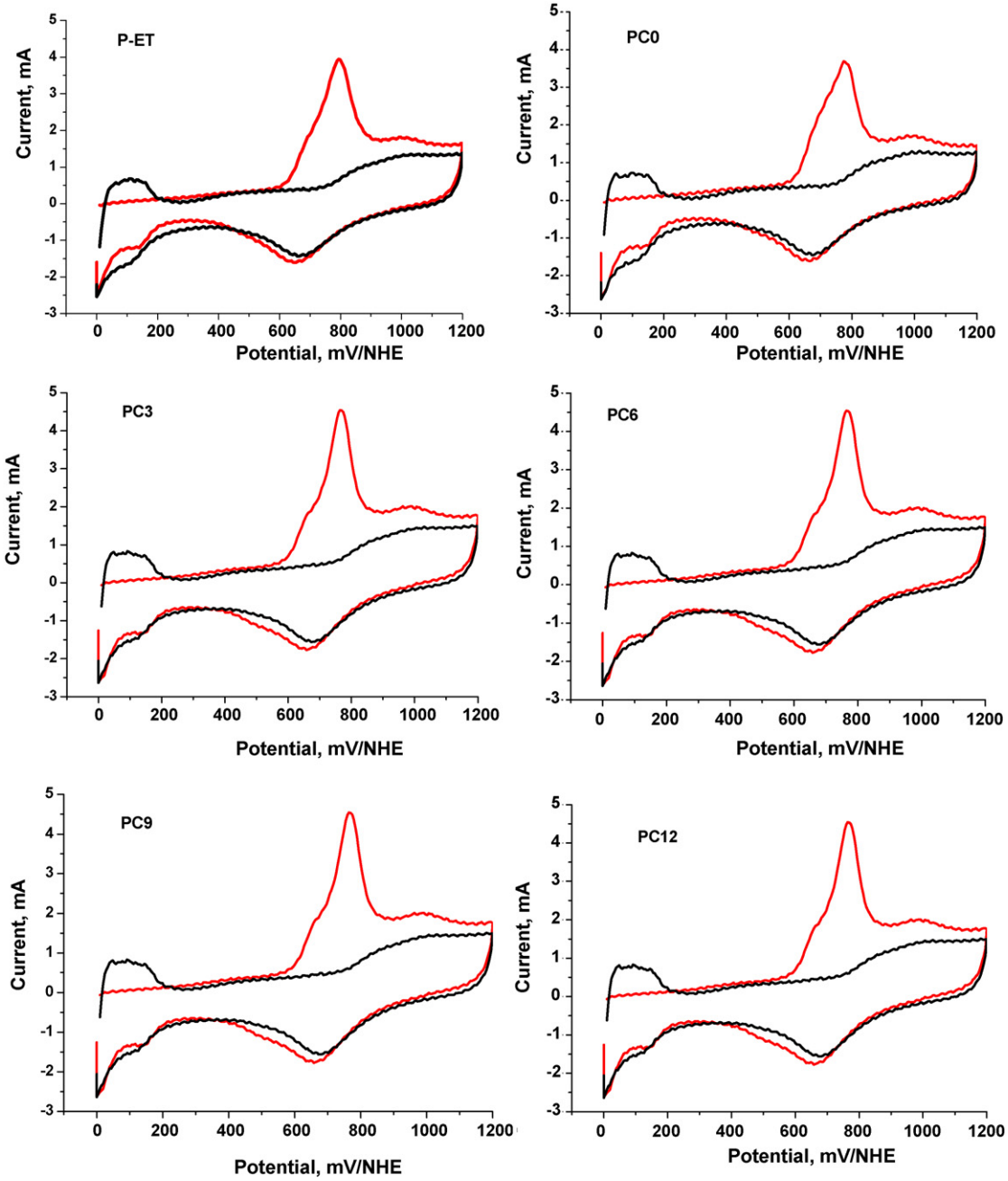

Fig. 4. CO-stripping curves of plain Pt and ceria incorporated Pt supported catalysts such as P-ET, PC0, PC3, PC6, PC9, PC12.

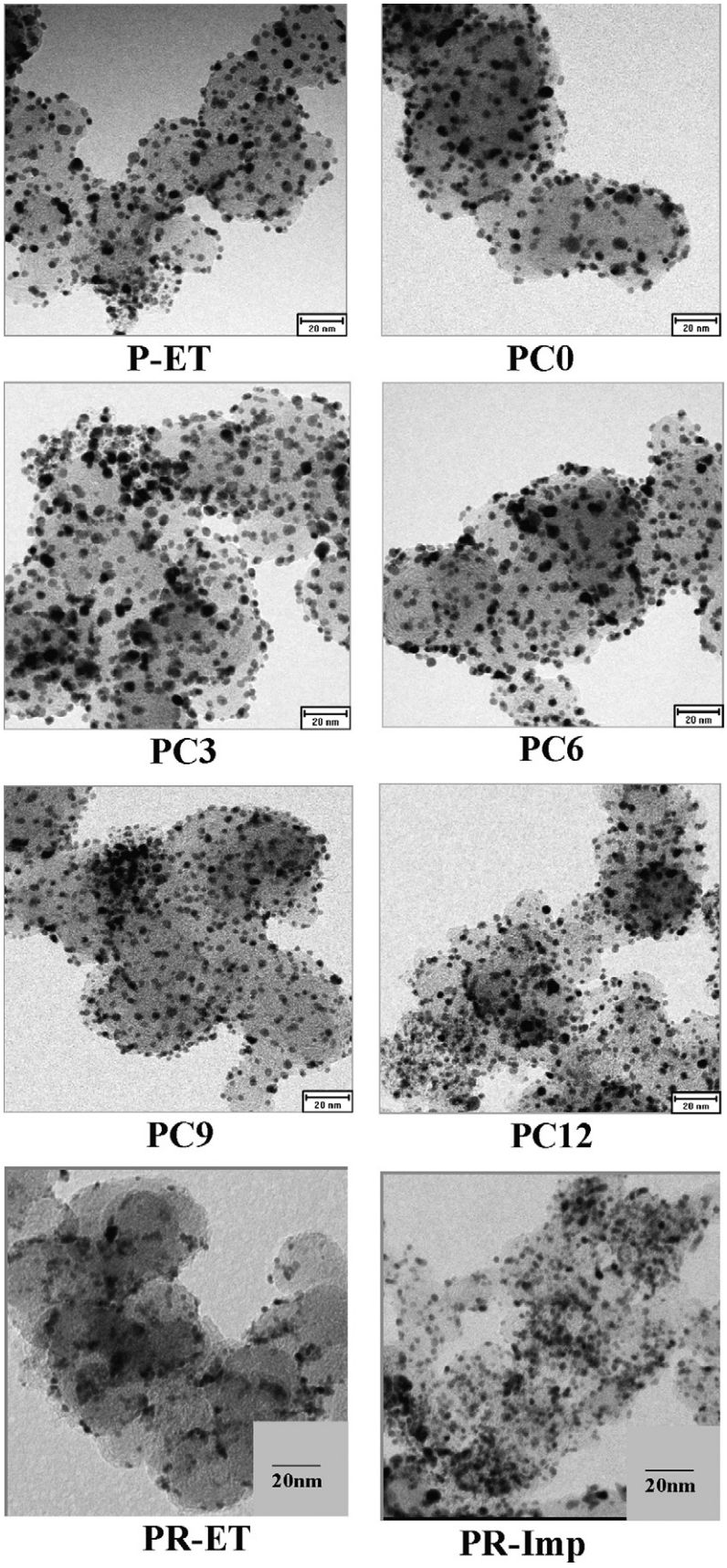

Fig. 5. Transmission electron micrographs of catalyst systems such as P-ET, PC0, PC3, PC6, PC9, PC12, PR-ET and PR-Imp.

X-ray diffractograms were made for $9CeO_2$/C, $12CeO_2$/C, Pt/C (E-Tek), PC0, and all ceria incorporated Pt/C under this study. The crystallite size of metallic particulates of catalysts is given in Table 2. A few representative XRD patterns are shown in Fig. 6. In Pt/C as well as Pt-CeO_2/C catalysts, the characteristic diffraction peaks of the face centered cubic crystalline (fcc) Pt, namely (1 1 1), (2 0 0), (2 2 0), (3 1 1) and (2 2 2) in the regions of 39.76, 46.24, 67.45, 81.28 and 87.00 (2θ) demonstrate the presence of Pt in metallic form [58]. A small peak at 28.4 is indicative of ceria in case with $9CeO_2$/C. The peaks in the regions of 28.4 and 47.5 can be indexed for CeO_2 with fluorite structure. However, there is no shift in any of the diffraction peaks of platinum metal at all compositions indicating that the added CeO_2 is not playing any role in influencing the crystallographic orientations of platinum catalyst particles supported on carbon. That is, there is no alloy formation between Pt and CeO_2. The particle size of catalyst systems measured from XRD is in consistent with those obtained by TEM measurements. Slight broadening of XRD peaks found with PC9 and PC12 compared to PC0 indicates the decrease in particle size of Pt in ceria incorporated catalysts compared to ceria free Pt catalyst, substantiating the TEM observations. The broadening in ceria incorporated platinum supported catalysts are, however, not prominent, may be because the difference among the particle sizes of the ceria incorporated and ceria free platinum catalyst systems lie within 1.0 nm range.

The pore size distribution curves of all the electrocatalysts under this study have been shown in Fig. 7. The specific surface area and pore characteristics of these systems are given in Table 4. A decrease in BET surface area of Pt/C with the incorporation of increased amount of ceria indicates that ceria is uniformly distributed on pores of carbon support. A gradual decrease in pore diameter of the catalyst systems below 2.5 nm were also noted with increased ceria content. It appears that ceria get deposited at the micropores of carbon support reducing the micorpore volumes in the carbon.

It is necessary to understand the influence of ceria and platinum interaction in the present systems. X-ray photoelectron spectroscopy (XPS) is a valuable tool to elucidate electronic properties of materials in addition to chemical state of information. The XPS traces of Pt/C system which is free from the ceria and the best performed ceria incorporated Pt-CeO_2/C system namely PC9 are shown in Fig. 8. Fig. 8a–d show the regional spectra of O_{1s} and $Pt_{4f7/2}$, and Fig. 8e shows the regional spectrum for Ce_{3d} of PC0 and PC9 catalyst systems. In PC0, there is only one O_{1s} peak centered at 532 eV with a small shoulder indicating the presence of oxygen

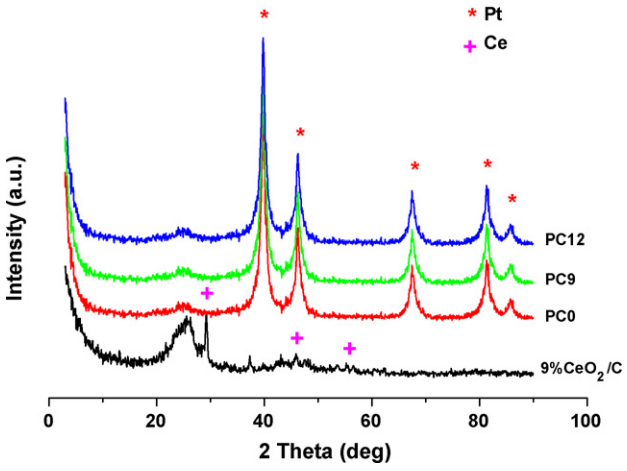

Fig. 6. X-ray diffraction patterns of 9% CeO_2/C, PC0, PC9 and PC12.

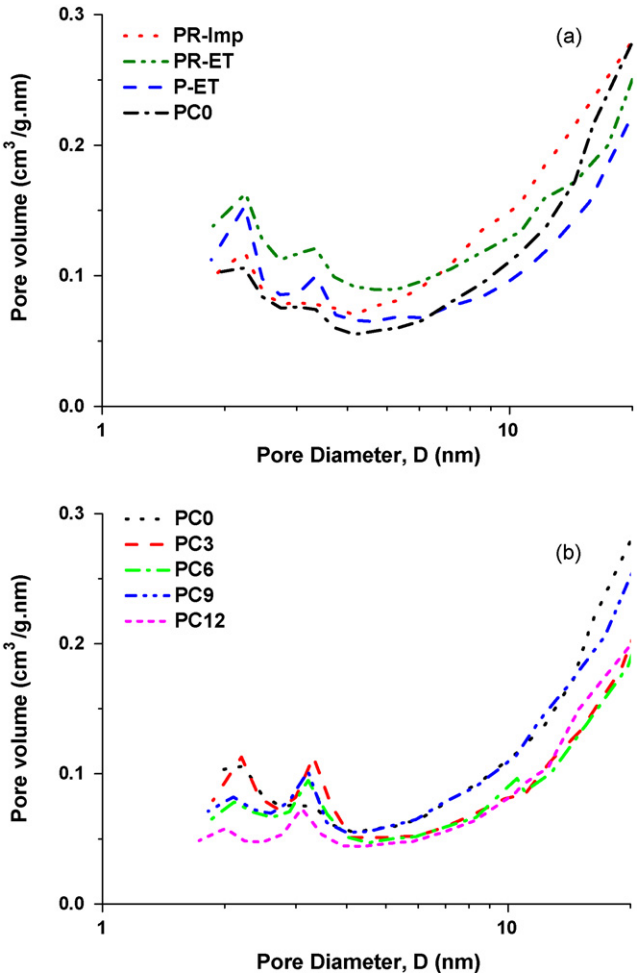

Fig. 7. Pore size distribution curves of catalyst systems (a) PR-Imp, PR-ET, P-ET and PC0 (b) PC0, PC3, PC6, PC9 and PC12.

species from carbon surface (–C═O) [59]. While in case of PC9, the O_{1s} oxygen peak in the region between 528–537 eV appears as doublet indicating the presence of two kinds of oxygen species which originate from two different chemical species namely carbon surface and ceria.

The regional spectra were deconvoluted and the results are summarized in Table 4. Depending on the oxidation state of Pt, there are 2 or 3 sets of platinum peaks [59]. The most intense ones, located around 71 and 75 eV, are due to metallic platinum: $Pt_{4f7/2}$ and $Pt_{4f5/2}$. The positions of these peaks are affected by the interactions between Pt and C. A shift in the binding energy (BE) of the supported Pt crystallites ($Pt_{4f7/2}$ at 71 eV) compared to bulk metallic Pt, 70.9 eV [60–66] has been attributed to metal support interaction. The second set of Pt signals appears at around 72.4–73.7 eV may be assigned to the presence of PtO or $Pt(OH)_2$, and the

Table 4
BET surface areas and pore volumes of the catalysts

Catalyst	BET (m^2/g)	Pore volume (cm^3/g)
P-ET	129	0.345
PC0	136	0.347
PC3	91	0.335
PC6	84	0.296
PC9	76	0.295
PC12	63	0.279
PR-Imp	144	0.387
PR-ET	163	0.372

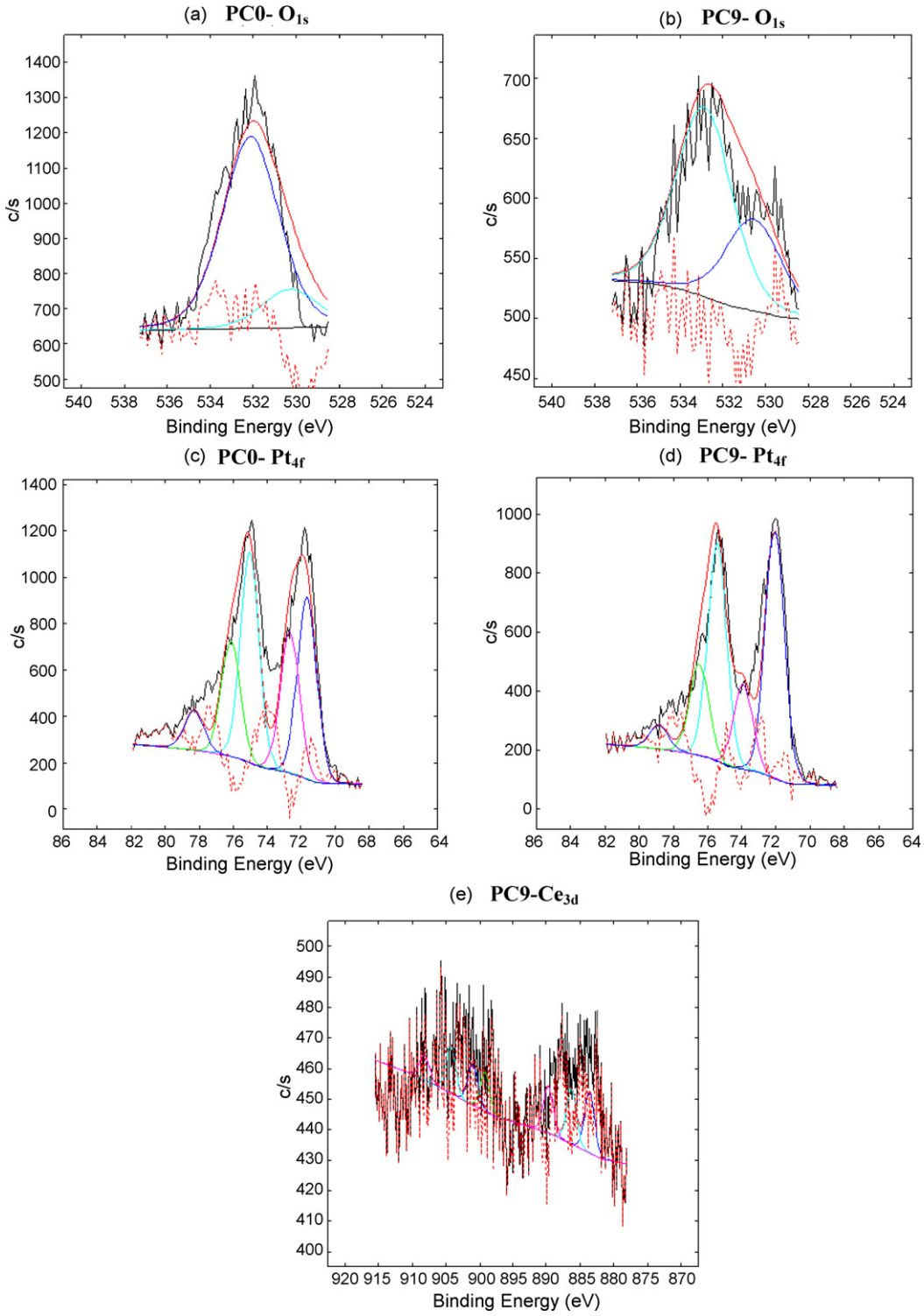

Fig. 8. XPS Spectra for O_{1s} region of PC0 and PC9, Pt_{4f} core level region of PC0 and PC9, and Ce_{3d} core level region of PC9.

low intense third set is expected at 74.3–76.2 eV may be attributed to PtO_2 [59].

From Table 5, it is clear that Pt is mainly present in its metallic form in both PC0 and with PC9. In PC0, 57% of metallic state of Pt and in PC9, 70% of metallic state of Pt is found. Compared to Pt/C (PC0) catalyst, the amount of Pt oxides decreased notably in the ceria containing Pt-CeO_2 (PC9) catalyst system. It appears that in ceria incorporated Pt/C systems, the Pt ions should have been reduced by Ce^{3+} during the preparation steps through the following redox reactions [67]:

$$Pt^{4+} + 4Ce^{3+} \rightarrow Pt + 4Ce^{4+} \quad \text{and/or}$$

$$Pt^{2+} + 2Ce^{3+} \rightarrow Pt + 2Ce^{4+}$$

As a result, the reduced Pt crystallites finely disperse and adhere to ceria particles deposited on carbon support.

Table 5
XPS data of the catalysts

Catalyst	Peak	Binding energy (eV)	Species	Relative ratio (%)
PC0	Pt_{4f}	71.63	Pt	57
		75.03	Pt	
		72.64	PtO, $Pt(OH)_2$	37.2
		76.16	PtO, $Pt(OH)_2$	
		78.13	PtO_2	5.8
PC9	Pt_{4f}	72.05	Pt	70
		75.45	Pt	
		73.90	PtO, $Pt(OH)_2$	26.5
		76.52	PtO, $Pt(OH)_2$	
		78.85	PtO_2	3.5
	Ce_{3d}	883.6	CeO_2	65
		889.71	CeO_2	
		899.25	CeO_2	
		901.04	CeO_2	
		886.28	Ce_2O_3	35
		904.02	Ce_2O_3	

Concerning Ce_{3d}, the peaks at 886.28 and 904.02 eV are typical of Ce^{3+}, while the main features of Ce^{4+} are at 883.60, 889.71, 889.25 and 901.04 eV [68]. The percentage composition of Ce^{3+} is 65% while that of Ce^{4+} is 35%. The existence of Ce^{3+} proves that part of Ce^{4+} is in reduced form, that is, Ce exists in form of multivalent state in the catalysts. One can see lots of noise in the Ce_{3d} spectrum of the catalyst system with the composition 40 wt% Pt-9 wt% CeO_2/C. It was very difficult for us to obtain a refined XPS spectrum for Ce in the Pt-CeO_2 supported on carbon in spite of our repeated attempts for the chosen catalyst composition. This might be due to relatively low amount of nano-size ceria particles dispersed on porous carbon support.

We propose a tentative reaction mechanism for the methanol electrooxidation on Pt-CeO_2/C catalysts as follows. The methanol is converted into CO_2 on Pt catalysts by a six electrons process. This leads to the formation of strongly adsorbed linearly bound CO as surface species leading to self-poisoned Pt catalysts. The surface oxygen of ceria may oxidize the CO on the surface of Pt. This is a kind of bifunctional mechanism [1,3,13,69–75].

$$CeO_2 + H_2O \rightarrow CeO_2\text{-}OH_{ads} + H^+ + e^-$$

$$Pt{-}CO_{ads} + CeO_2\text{-}OH_{ads} \rightarrow Pt + CeO_2 + CO_2 + H^+ + e^-$$

and/or

$$Pt\text{-}CeO_2 + xCO \rightarrow Pt{-}CeO_{2-x} + xCO_2$$

It appears that the enhancement is likely to occur at the interface of Pt and ceria in these supported systems.

Cyclic voltammetric studies (Fig. 1) as well as chronoamperometry (Fig. 2) results reveal that ceria incorporated platinum supported catalysts exhibit enhanced activity towards methanol electro-oxidation compared to platinum supported catalysts and this inference is further confirmed by EIS results (Fig. 3). According to Wang et al. [76], the methanol electro-oxidation current can be enhanced by two ways. One way is by improving the electro-oxidizing kinetics of CO species on Pt through bi-functional mechanism and another way is to increase the mass transfer rates of reactants (such as methanol) and products (such as CO_2) by stirring or by increasing large pores in catalyst layer. In the present investigation, since certain amounts of voids were filled by CeO_2 nanoparticles as indicated by BET surface area as well as decreased pore volume and pore diameter of the catalysts with increased ceria addition (Fig. 7), the amounts of large pores would not be increased by ceria addition and hence the mass transfer in catalyst layer would less possibly be improved by ceria incorporation. Hence, the most probable reason might be the improved methanol electro-oxidation kinetics by CeO_2. CO-stripping results (Fig. 4) indicate the facile removal of intermediate poisoning species CO in the presence of CeO_2.

Mamontov et al. [77] suggest the presence of 4f electrons in the ground state of CeO_2 due to f-p hybridization, so the electron transition to 3d orbital of Pt becomes easy and hence this may facilitate the removal of CO. In other words, electron effect of Ce atom in ceria can change the electron structure of Pt catalysts, weakening the adsorption intensity of CO and reduce the CO coverage on the surface of the catalysts. The CO that desorbs from Pt can be readily oxidized by the surface oxygen of ceria. It is presumed that both intrinsic and bifunctional mechanism may coexist in the Pt-ceria system for methanol electrooxidation. The mechanistic routes are highly speculative at this stage because it is hard for us to maintain a well-defined surface composition with supported systems. Efforts are underway to make unsupported as well as supported highly active alloy/binary mixtures of Pt-CeO_2 with well-characterized surface composition prepared via various other preparation routes. Such a study may help us to unequivocally elucidate and establish the mechanistic steps.

4. Conclusions

Present investigation reveals that the catalytic activity of Pt/C catalyst can be promoted by the incorporation of ceria towards methanol electrooxidation and hence ceria acts as a co-catalyst with Pt. The promotion by ceria has been realized at an optimum composition namely 40 wt% Pt-9 wt% CeO_2/C, which exhibited higher methanol electrooxidation activity than 40 wt% Pt/C. The influence of ceria on platinum activity towards methanol oxidation may be due to both bifunctional as well as intrinsic mechanism. Pt-CeO_2 alloy system appears to be a promising and less expensive methanol oxidation anode catalyst. Efforts are fostered in tailoring the present catalyst system and understanding surface site interactions.

Acknowledgements

This work was financially supported by the Korean Ministry of Commerce, Industry and Energy through the Institute of Industrial Technology Evaluation and Planning (ITEP) under the research program: Development of Core Technologies for Next Generation Fuel Cells. One of the authors, Dr. M. Aulice Scibioh, thanks the Korean Federation of Science and Technology Societies (KOFST) and Korea Science and Engineering Federation (KOSEF) for support and assistance through the Brain Pool Program.

References

[1] M.P. Hogarth, G.A. Hards, Platinum Metal Rev. 40 (1996) 150–159.
[2] G.T. Burstein, C.J. Barnett, A.R. Kucernak, K.R. Williams, Catal. Today 38 (1997) 425–437.
[3] A. Hamnet, Catal. Today. 38 (1997) 445–457.
[4] P. Costamagna, S. Srinivasan, J. Power Sources 102 (2001) 242–252.
[5] E. Antolini, Mater. Chem. Phys. 78 (2003) 563–573.
[6] E. Antolini, J. Appl. Electrochem. 34 (2004) 563–576.
[7] Y.Y. Tong, H.S. Kim, P.K. Babu, P. Waszczuk, A. Wieckowski, E. Oldfield, J. Am. Chem. Soc. 124 (2002) 468–473.
[8] T.J. Schmidt, M. Noeske, H.A. Gasteiger, R.J. Behm, P. Britz, W. Brijoux, H. Bönnemann, Langmuir 13 (1997) 2591–2595.
[9] Y. Takasu, T. Fujiwara, Y. Murakami, K. Sasaki, M. Oguri, T. Asaki, W. Sugimoto, J. Electrochem. Soc. 147 (2000) 4421–4427.
[10] Y.M. Liang, H.M. Zhang, B.L. Yi, Z.H. Zhang, Z.C. Tan, Carbon 43 (2005) 3144–3152.
[11] V. Radmilović, H.A. Gasteiger, P.N. Ross Jr., J. Catal. 154 (1995) 98–106.
[12] C. Bock, C. Paquet, M. Couillard, G.A. Botton, B.R. MacDougall, J. Am. Chem. Soc. 126 (2004) 8028–8037.
[13] H.A. Gasteiger, N. Marković, P.N. Ross Jr., E.J. Cairns, J. Phys. Chem. 98 (1994) 617–625.

[14] B. Yang, Q. Lu, Y. Wang, L. Zhuang, J. Lu, P. Liu, J. Wang, R. Wang, Chem. Mater. 15 (2003) 3552–3557.
[15] G.A. Camara, M.J. Giz, V.A. Paganin, E.A. Ticianelli, J. Electroanal. Chem. 537 (2002) 21–29.
[16] G. Samjeské, H. Wang, T. Löffler, H. Baltruschat, Electrochim. Acta 47 (2002) 3681–3692.
[17] M. Götz, H. Wendt, Electrochim. Acta 43 (1998) 3637–3644.
[18] P. Shen, K. Chen, A.C.C. Tseung, J. Electrochem. Soc. 142 (1995) L85–L86.
[19] D.C. Papageorgopoulos, M. Keijzer, F.A. de Bruijn, Electrochim. Acta 48 (2002) 197–204.
[20] K.W. Park, J.H. Choi, B.K. Kwon, S.A. Lee, Y.E. Sung, H.Y. Ha, S.A. Hong, H. Kim, A. Wieckowski, J. Phys. Chem. B 106 (2002) 1869–1877.
[21] T.C. Deivaraj, W. Chen, J.Y. Lee, J. Mater. Chem. 13 (2003) 2555–2560.
[22] K.W. Park, J.H. Choi, B.K. Kwon, S.A. Lee, C. Pak, H. Chang, Y.E. Sung, J. Catal. 224 (2004) 236–242.
[23] H.R. C-Mercado, H. Kim, B.N. Popov, Electrochem. Commun. 6 (2004) 795–799.
[24] P. Piela, C. Eickes, E. Brosha, F. Garzon, P. Zelenay, J. Electrochem. Soc. 151 (2004) A2053–A2059.
[25] T. Iwasita, H. Hoster, A. John-Anacker, W.F. Lin, W. Vielstich, Langmuir 16 (2000) 522–529.
[26] M.B. Oliveira, L.P.R. Profeti, P. Olivi, Electrochem. Commun. 7 (2005) 703–709.
[27] L.D. Burke, O.J. Murphy, J. Electroanal. Chem. 101 (1979) 351–361.
[28] K. Lasch, L. Jorissen, J. Garche, J. Power Sources 84 (1999) 225–230.
[29] Z. Jusys, T.J. Schmidt, L. Dubau, K. Lasch, L. Jorissen, J. Garche, R.J. Bhem, J. Power Sources 105 (2002) 297–304.
[30] L.X. Yang, C. Bock, B. MacDougall, J. Park, J. Appl. Electrochem. 34 (2004) 427–438.
[31] K.-W. Park, J.-H. Choi, K.-S. Ahn, Y.-E. Sung, J. Phys. Chem. B. 108 (2004) 5989–5994.
[32] Q. Fu, M. F-Stephanopoulos, Science 301 (2003) 935–938.
[33] C. Perkins, M. Henderson, C. Peden, G. Herman, J. Vac. Sci. Technol. A 19 (2001) 1942–1946.
[34] P. Bera, A. Gayen, M.S. Hegde, N.P. Lalla, L. Spadaro, F. Frusteri, F. Arena, J. Phys. Chem. B 107 (2003) 6122–6130.
[35] H.B. Yu, J.-H. Kim, H.-I. Lee, M.A. Scibioh, J. Lee, J. Han, S.P. Yoon, H.Y. Ha, J. Power Sources 140 (2005) 59–65.
[36] C.W. Xu, P.K. Shen, Chem. Commun. (2004) 2238–2239.
[37] C.W. Xu, P.K. Shen, J. Power Sources 142 (2005) 27–29.
[38] C.L. Campos, C. Roldan, M. Aponte, Y. Ishikawa, C.R. Cabrera, J. Electroanal. Chem. 581 (2005) 206–215.
[39] J.W. Guo, T.S. Zhao, J. Prabhuram, R. Chen, C.W. Wong, J. Power Sources 156 (2006) 345–354.
[40] A. Holmgren, B. Andersson, J. Catal. 178 (1998) 14–25.
[41] A. Pozio, M.D. Francesco, A. Cemme, F. Cardellini, L. Giorgi, J. Power Sources 105 (2002) 13–19.
[42] M. Ciureanu, H. Wang, J. Electrochem. Soc. 146 (1999) 4031–4040.
[43] M.J. Weaver, S.C. Chang, L.W.H. Leung, X. Jiang, M. Rubel, M. Szklarczyk, D. Zurawski, A. Wieckowski, J. Electroanal. Chem. 327 (1992) 247–260.
[44] J.M. Feliu, J.M. Orts, A. F-Vega, J. Clavillier, J. Electroanal. Chem. 296 (1990) 191–201.
[45] X. Zhang, K.-Y. Chan, J. Mater. Chem. 12 (2002) 1203–1206.
[46] W.Y. Yu, W.X. Tu, H.F. Liu, Langmuir 15 (1999) 6–9.
[47] M.L. Anderson, R.M. Storud, D.R. Rolison, Nano Lett. 2 (2002) 235–240.
[48] J.-F. Drillet, A.E.J. Friedemann, R. Kotz, B. Schnyder, V.M. Schmidt, Electrochim. Acta 47 (2002) 1983–1988.
[49] R. Manohara, J.B. Goodenough, J. Mater. Chem. 2 (1992) 875–887.
[50] Z. Liu, X.Y. Ling, X. Su, J.Y. Lee, J. Phys. Chem. B. 108 (2004) 8234–8240.
[51] T.C. Deivaraj, J.Y. Lee, J. Power Sources 142 (2005) 43–49.
[52] G.Q. Lu, W. Chrzanowski, A. Wieckowski, J. Phys. Chem. B 104 (2000) 5566–5572.
[53] J.-H. Kim, H.Y. Ha, I.-H. Oh, S.-A. Hong, H.N. Kim, H.-I. Lee, Electrochim. Acta 50 (2004) 801–806.
[54] A. Tschope, J.Y. Ying, H.L. Tuller, Sens. Actuators B 31 (1996) 111–114.
[55] J.T. Müller, P.M. Urban, W.F. Hölderich, J. Power Sources 84 (1999) 157–160.
[56] I.-M. Hsing, X. Wang, Y.-J. Leng, J. Electrochem. Soc. 149 (2002) A615–A621.
[57] Y.-C. Liu, X.-P. Qiu, W.-T. Zhu, G.-S. Wu, J. Power Sources 114 (2003) 10–14.
[58] C. He, H.R. Kunz, J.M. Fenton, J. Electrochem. Soc. 144 (1997) 970–979.
[59] V. Alderucci, L. Pino, P.L. Antonucci, W. Roh, J. Cho, H. Kim, D.L. Cocke, V. Antonucci, Mater. Chem. Phys. 41 (1995) 9–14.
[60] K.S. Kim, N. Winograd, R.E. Davis, J. Am. Chem. Soc. 93 (1971) 6296–6297.
[61] G.C. Allen, P.M. Tucker, A. Capon, R. Parsons, J. Electroanal. Chem. 50 (1974) 335–343.
[62] T. Dickinson, A.F. Povey, P.M.A. Sherwood, J. Chem. Soc., Faraday Trans. I 71 (1975) 298–311.
[63] M. Peuckert, F.P. Coenen, H.P. Bonzel, Electrochim. Acta 29 (1984) 1305–1314.
[64] E.T. Wagner, P.N. Ross, Appl. Surf. Sci. 24 (1985) 87–107.
[65] E. Rach, J. Heitbaum, Electrochim. Acta 31 (1986) 477–479.
[66] B.J. Kennedy, A. Hamnett, J. Electroanal. Chem. 283 (1990) 271–285.
[67] S.-Y. Huang, C.-M. Chang, C.-T. Yeh, J. Catal. 241 (2006) 400–406.
[68] F. Giordano, A. Trovarelli, C. de Leitenburg, M. Giona, J. Catal. 193 (2000) 273–282.
[69] J.B. Goodenough, A. Hamnett, B.J. Kennedy, R. Manoharan, S.A. Weeks, J. Electroanal. Chem. 240 (1988) 133–145.
[70] D. Chu, S. Gilman, J. Electrochem. Soc. 143 (1996) 1685–1690.
[71] V. Radmilovic, H.A. Gasteiger, P.N. Ross Jr., J. Catal. 154 (1995) 98–106.
[72] H.A. Gasteiger, P.N. Ross Jr., E.J. Cairns, Surf. Sci. 293 (1993) 67–80.
[73] H.A. Gasteiger, N. Markovic, P.N. Ross Jr., E.J. Cairns, J. Phys. Chem. 97 (1993) 12020–12029.
[74] M. Watanabe, S. Motoo, J. Electroanal. Chem. 60 (1975) 267–273.
[75] A. Kabbabi, R. Faure, R. Durand, B. Bedan, F. Hahn, J.-M. Leger, C. Lamy, J. Electroanal. Chem. 444 (1998) 41–53.
[76] J. Wang, X. Deng, J. Xi, L. Chen, W. Zhu, X. Qiu, J. Power Sources 170 (2007) 297–302.
[77] E. Mamontov, W. Dmowski, T. Egami, C.-C. Kao, J. Phys. Chem. Solids. 61 (2000) 431–433.